



Article

A Comparative Genomics Approach for Analysis of Complete Mitogenomes of Five Actinidiaceae Plants

Jun Yang^{1,†}, Chengcheng Ling^{1,†}, Huamin Zhang¹, Quaid Hussain² , Shiheng Lyu², Guohua Zheng^{3,*} and Yongsheng Liu^{1,*} 

¹ College of Horticulture, Anhui Agriculture University, Hefei 350002, China

² State Key Laboratory of Subtropical Silviculture, Zhejiang A&F University, 666 Wusu Street, Hangzhou 311300, China

³ College of Horticulture, Fujian Agriculture and Forestry University, Fuzhou 350002, China

* Correspondence: fafuzgh@126.com (G.Z.); liuyongsheng1122@ahau.edu.cn (Y.L.)

† These authors equally contributed to this work.

Abstract: Actinidiaceae, an economically important plant family, includes the *Actinidia*, *Clematoclethra* and *Saurauia* genus. Kiwifruit, with remarkably high vitamin C content, is an endemic species widely distributed in China with high economic value. Although many Actinidiaceae chloroplast genomes have been reported, few complete mitogenomes of Actinidiaceae have been studied. Here, complete circular mitogenomes of the four kiwifruit species and *Saurauia tristyla* were assembled. Codon usage, sequence repeats, RNA editing, gene transfers, selective pressure, and phylogenetic relationships in the four kiwifruit species and *S. tristyla* were comparatively analyzed. This research will contribute to the study of phylogenetic relationships within Actiniaceae and molecular barcoding in kiwifruit.

Keywords: Actinidiaceae; mitogenome; comparative analysis; phylogenetic analysis



Citation: Yang, J.; Ling, C.; Zhang, H.; Hussain, Q.; Lyu, S.; Zheng, G.; Liu, Y. A Comparative Genomics Approach for Analysis of Complete Mitogenomes of Five Actinidiaceae Plants. *Genes* **2022**, *13*, 1827. <https://doi.org/10.3390/genes13101827>

Academic Editor: Zhiqiang Wu

Received: 28 August 2022

Accepted: 1 October 2022

Published: 9 October 2022

Publisher's Note: MDPI stays neutral with regard to jurisdictional claims in published maps and institutional affiliations.



Copyright: © 2022 by the authors. Licensee MDPI, Basel, Switzerland. This article is an open access article distributed under the terms and conditions of the Creative Commons Attribution (CC BY) license (<https://creativecommons.org/licenses/by/4.0/>).

1. Introduction

According to the endosymbiosis theory, the mitochondrion is an endosymbiotic alphaproteobacterium engulfed by the archaeal-derived host cell and eventually evolves into a semiautonomous organelle [1–3]. Mitochondria, known as energy factories, play a crucial role in numerous metabolic processes related to energy generation, synthesis, and degradation in living cells [4]. Mitochondrial DNA is maternally inherited in most seed plants [5]. With genome sequencing technology's rapid development, various complete organelle genomes in plants have been extensively studied [6]. Nearly 7576 chloroplasts and mitogenomes of land plants have been published in the National Center for Biotechnology Information (<https://www.ncbi.nlm.nih.gov/genome/browse#!/organelles/>) (accessed on 10 January 2022). The number of mitogenomes in land plants published was less than 20 before 2015 (Supplementary Figure S1). In recent years, it is no doubt that the number of land plant mitogenomes has increased significantly from 2018 to 2021 (Supplementary Figure S1). However, compared to the completed chloroplast genomes (7246), only 324 completed mitogenomes were assembled (Supplementary Table S1), suggesting that the interpretation and functional annotation of the mitochondrial genome is complex in comparison to other organelles.

The intergenomic DNA transfers and highly dynamic, multipartite structures of plant mitogenomes may make it challenging to build plant mitogenomes [7]. Several articles have reported that most plant mitogenomes range from 200 to 2000 kb in size [8]. Differences in mitogenome size can be attributed to repetitive sequences and foreign DNA derived from other organisms during evolution [9]. Many intramolecular recombination events and subgenomic conformations have been found in some land plants, such as *Scutellaria tsinyunensis* [10], *Cucumis sativus* [11], *Ipomoea batatas* [12], and *Brassica napus* [13]. In extreme environments, gene loss and RNA edits may occur during plant mitogenome

rearrangement [14]. Several separate chromosomes can be found in some higher plant mitochondrial genomes. The cucumber mitogenome, for instance, has three separate chromosomes [11]. The mitogenomes of *Globodera ellingtonae* and *Camellia sinensis* have two separate chromosomes [15,16]. The mitogenomes of the plant's seeds contain many repeating sequences, including simple sequence repeats (SSRs), tandem repeats, and scattered repeats. In addition, there are also many insertions/deletions (indels) and single nucleotide polymorphisms (SNPs) within mitogenomes [17,18]. SSRs and SNPs have been widely applied to identify species rapidly and for phylogenetic plant analyses, especially in Chinese herbal medicine classification [19,20]. Moreover, it is an essential feature for mitogenome evolution via intracellular transfer between the mitochondria and the chloroplast genomes [21]. Most of the transferred sequences are transferred from the nucleus to the mitochondria, but several chloroplast-derived tRNA genes are transferred to the mitochondria and perform essential functions [22]. The horizontal gene transfer (HGT) phenomenon also plays a significant role in the evolution of plant mitogenomes [9]. These findings suggested the existence of instability in higher plants' mitogenome structures. Finally, a long-reads strategy in combination with short-reads technologies (Pacbio SMRT, Oxford Nanopore, or Illumina mate-pair) were applied to solve the problem caused by this structural instability in mitogenome assembly.

Actinidiaceae, an economically important plant family, includes the *Actinidia*, *Clematoclethra*, and *Saurauia* genus [23,24]. Among the Actinidiaceae family of the Asterids, kiwifruit with remarkably high vitamin C content, commonly known as 'the king of fruits', is an economically important horticultural fruit tree. Kiwifruit is widely cultivated in Asia, Europe and Oceania (<https://www.fao.org/faostat/zh/#data/QCL>, Supplementary Figure S2) (accessed on 3 December 2021). Worldwide annual kiwifruit production increased rapidly from 2012 to 2020 and reached approximately 2 million tons in 2020 (<https://www.fao.org/faostat/zh/#data/QCL>, Supplementary Figure S3) (accessed on 3 December 2021). Total kiwifruit production in Asia was the highest, accounting for 52.5%, followed by Europe (25.3%) from 2012 to 2020 (<https://www.fao.org/faostat/zh/#data/QCL>, Supplementary Figure S4) (accessed on 3 December 2021). It is noted that the annual kiwifruit production in China was the highest in Asia and reached up to 1.49 million tons in 2020 (<https://www.fao.org/faostat/zh/#data/QCL>, Supplementary Figure S5) (accessed on 3 December 2021). This may be due to the abundant kiwifruit germplasm resources in China. So far, diploid *A. chinensis* and hexaploid *A. chinensis* var *deliciosa* are the most commercial kiwifruit varieties. Abiotic and biotic stresses, including drought, salinity, low or high temperatures, and *Pseudomonas syringae* pv. *actinidiae* (Psa) seriously affect the yield and quality of kiwifruit [25]. After incidence of Psa, there is no remedy available to control it, except for destroying the tree to prevent the spread of the disease. Thus, Psa seriously threatens the production and development of the kiwifruit industry worldwide. It has been reported that *A. eriantha* var 'huate' and *A. chinensis* var *deliciosa* 'jinkui' strongly resist Psa [26,27]. Mitochondria genetic engineering would be beneficial in developing a method of resilience to abiotic and biotic stresses [25]. Hence, the complete mitogenomes of kiwifruit are sequenced, providing great promise for breeding kiwifruit cultivars with resilience to abiotic and biotic stresses.

For the last three decades, 4 kiwifruit nuclear genomes and over 29 complete chloroplast genomes from the Actinidiaceae family have been sequenced [28–32], while no complete mitogenome of this family has been reported previously. To elucidate the evolutionary mechanisms and structural features that underlie the Actinidiaceae family's mitogenomic diversity, the complete mitochondria genome of the diploid *A. chinensis*, and the tetraploid *A. chinensis*, hexaploid *A. chinensis* var *deliciosa*, *A. eriantha* and *S. tristyla* were sequenced and assembled in this study. The mitochondria genome with a two-chromosomal conformation was found in diploid *A. chinensis*, tetraploid *A. chinensis* and *S. tristyla*. The genome size (939 kb) of *A. chinensis* var *deliciosa* was significantly more extensive than other Actiniaceae species. Therefore, we hypothesized that the mitogenome may experience expansion during *A. chinensis* ploidy doubling. We analyzed the mitogenome structures of

four kiwifruit species and *S. tristyla* to elucidate/unveil the genomic repeats, RNA editing sites, relative synonymous codon usage, gene transfer, and the evolutionary relationships among the Actinidiaceae family. To sum up, our study will be instrumental for genetic engineering and breeding programs.

2. Materials and Methods

2.1. Plant Materials and Genome Sequencing

Table S3 shows details of the tested materials. Fresh leaves were wrapped in aluminum foil, flash frozen in liquid nitrogen, and stored at -80°C for subsequent use. High-quality total genomic DNA was extracted using a DNAsure Plant Kit (Tiangen Biotech, Co. Ltd., Beijing, China). The DNA library construction and sequencing were performed as previously reported by Emerman et al. [33].

2.2. Mitogenome Assembly and Annotation

The Oxford Nanopore long-reads were de novo assembled for the five mitogenomes using SMARTdenovo with default parameters [34]. To obtain high-quality mitogenomes, the Illumina short-reads were conducted after polishing with minimap2/miniasm [35], racon (v1.4.20) [36] and pilon (v1.23) [37] to correct nanopore long-read errors. Furthermore, we used the BWA [38] and SAMtools [39] to map all the raw reads to the assemble mitogenomes. In the last step, the assembled PacBio sequences were checked for overlaps and joined. Mitochondria annotations were achieved using the online Geseq tool [40] with *Actinidia arguta* as the reference mitogenomes from GenBank:MH559343. We manually edited the annotation problems, using Apollo [41], and OGDRAWv1.3.1 [42] to draw the circular maps of the mitogenomes. All transfer RNA genes were checked by the online tRNAscanSE service (<http://lowelab.ucsc.edu/tRNAscan-SE/>, accessed on 1 January 2022) [43].

2.3. Repeat Sequences and Chloroplast to Mitochondrion DNA Transformation

The SSR (simple sequence repeats), including mono-, di-, tri-, tetra-, penta-, and hexanucleotide bases pairs with 12, 6, 4, 3, 3, and 3 repeat numbers, respectively, were detected using the microsatellite identification tool MISA-web55 (<https://webblast.ipk-gatersleben.de/misa/>, accessed on 3 February 2022) with default parameters [44]. Tandem Repeats Finder v4.09 software [45] (<http://tandem.bu.edu/trf/trf.submit.options.html>, accessed on 5 February 2022) with default parameters was employed to detect tandem repeats (>6 bp repeat units). The chloroplast fragments' insertion in the mitogenome was identified using the BLASTN tool according to the following screening criteria: matching rate $\geq 70\%$, E-value $\leq 1 \times 10^{-6}$, and length ≥ 40 [46]. Circos maps were visualized using the advanced circos module in Tbttools [47].

2.4. RNA Editing Predicting and Codon Usage

We used the online PREP-Mt suite of servers (<http://prep.unl.edu/>, accessed on 5 March 2022) [48], with a cutoff value of 0.2, to predict the RNA editing sites of the 39 protein-coding genes of the 5 mitogenomes. The relative synonymous codon usage (RSCU) was calculated by MEGA X53 [49].

2.5. Substitution Rate Calculation and Phylogenetic Inference

Pairwise 19 protein-coding gene sequences of the mitogenomes of *Actinidia* were used to estimate the pairwise nucleotide substitution rates, including the non-synonymous substitution rate (K_a) and synonymous substitution rate (K_s), and the ratio of K_a to K_s . The K_a/K_s ratios were calculated by PAML (v4.9) [50] using the yn00 module with default parameters. The K_a/K_s values' heatmap was plotted using Tbttools [47]. In order to further analyze the phylogenetic position of the Actinidiaceae species, 23 plant mitogenomes from GenBank were downloaded for phylogenetic tree construction. A total of 20 orthologous mitochondrial genes were identified and extracted using PhyloSuite (v1.2.1) [51]. The corresponding nucleotide sequences were aligned using MAFFT (v7.450) [52] implemented

in PhyloSuite. The phylogenetic tree was constructed using the maximum likelihood (ML) method via RAxML v8.1.5 [53] with 1000 bootstrap replicates. Furthermore, the web iTOL (<https://itol.embl.de>, accessed on 8 April 2022) [54] was used to visualize the phylogenetic trees.

3. Results

3.1. Mitogenome Assembly, Annotation and Gene Features

The de novo assembly assembled five complete mitogenomes of Actiniaceae species. The de novo genome assembly yielded a single circular molecule for *A. chinensis* var *deliciosa* (939 kb) and *A. eriantha* (768 kb). In contrast, two distinct circular chromosomal genomes for *A. chinensis* (2 \times), *A. chinensis* (4 \times) and *S. tristyla* (Figure 1A–D and Supplementary Table S2) were reported. *A. chinensis* (2 \times) and *A. chinensis* (4 \times) mitogenomes exhibited similar genome size (916 kb vs. 907 kb). The genome size (939 kb) of *A. chinensis* var *deliciosa* was significantly more extensive than the other Actiniaceae species. *S. tristyla* (482 kb) has the smallest genome size among them. Interestingly, their mitogenomes, containing similar GC content, are about 46% (Supplementary Table S2). A comparison of the annotated genes in Actiniaceae revealed that the pseudogene *rps2* is absent in tetraploid and hexaploid *A. chinensis* (Supplementary Figure S2). The loss of the *sdh4* gene in the *A. arguta* mitochondrion genome was also notable (Supplementary Figure S2).

3.2. Repeat Sequences and Chloroplast-Derived Region Analysis

As shown in Figure 2A, a total of 49–124 tandem repeats were found in the Actiniaceae mitogenome. The number of tandem repeats, comprising between 10 and 20 bp in the *A. chinensis* (2 \times) mitogenome, was significantly lower for the other species. Compared to the tetraploid and hexaploid *A. chinensis*, the number ranged from 40 bp to 105 bp in diploid *A. chinensis*. About half of the tandem repeats ranged from 10 bp to 20 bp in kiwifruit, whereas most of the tandem repeats ranged from 41 bp to 105 bp in *S. tristyla*. *A. eriantha* contained the fewest tandem repeats. A wealth of SSRs was identified (Figure 2). SSRs in hexamers were discovered in all species except *S. tristyla* (Figure 2C). Nearly 78% of the SSRs belonged to monomers and dimers (Figure 2B). Tetramers and pentamer-nucleotide repeats were less frequent in the Actiniaceae mitogenome. *A. chinensis* mitogenomes contained a higher number of SSRs than those of *S. tristyla* and *A. eriantha*. *S. tristyla* had the lowest number of SSRs (Figure 2B).

Plastid-derived sequences were detected in five Actiniaceae species' mitogenomes. Three species of chloroplasts and mitogenomes have high and widespread homologies in *A. chinensis* (2 \times –6 \times) (Figure 3E). A total fragment length of 50–55 kb of the tandem repeats red transferred fragment, which accounts for about 1/3 of the chloroplast genome, was identified in the *A. chinensis* (2 \times –6 \times) mitogenome (Figure 3F). Plastid-derived sequences in *A. chinensis* (2 \times –6 \times) were significantly higher in number than in *A. eriantha* and *S. tristyla* (Figure 3F). Five intact chloroplast genes (*rpoC1*, *ndhB*, *rps7*, *rps19*, and *rpl23*) were transferred into the mitogenome in the *A. chinensis* (2 \times –6 \times) species (Supplementary Table S2).

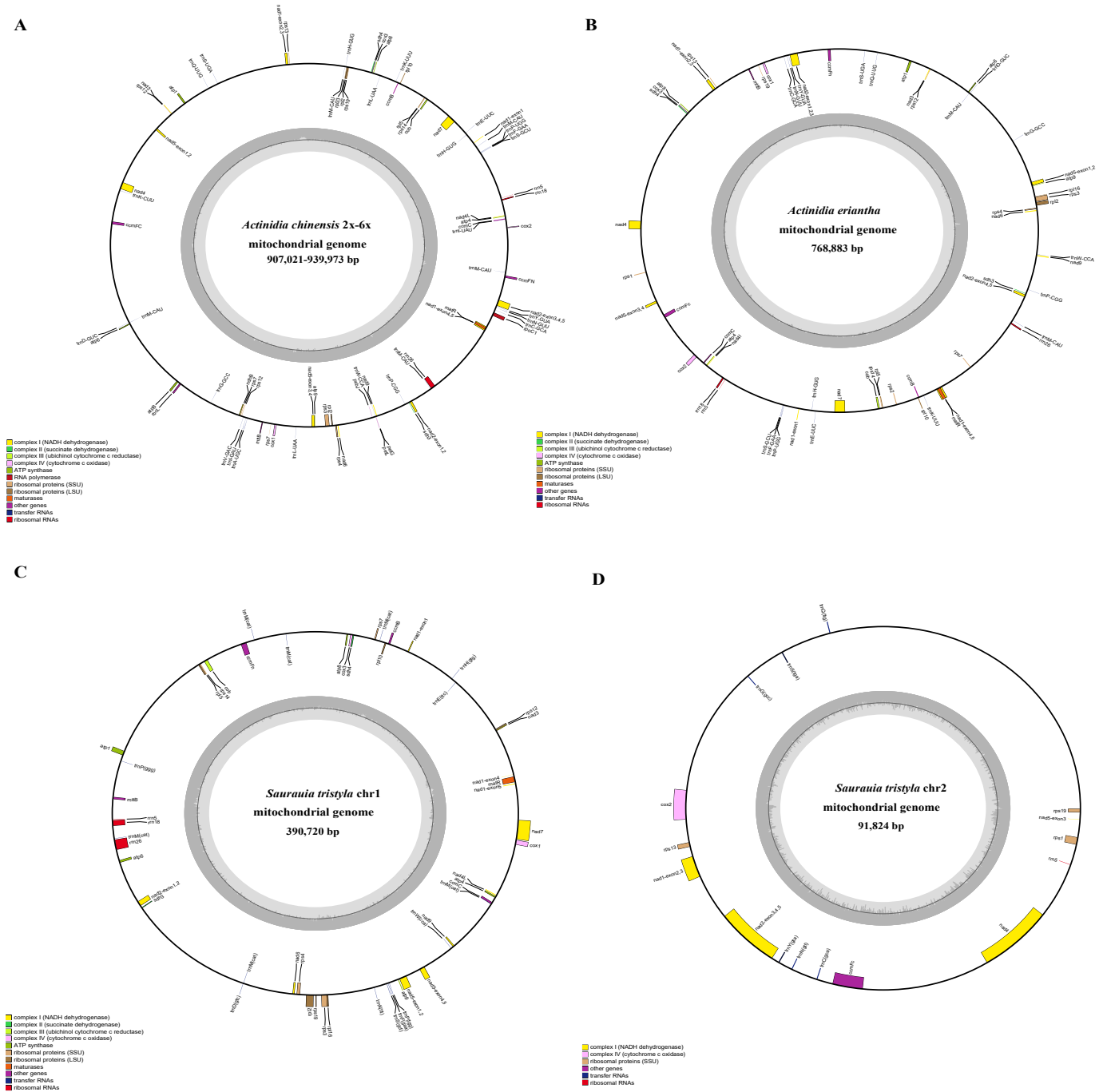


Figure 1. (A–D) Gene map of four kiwifruit species (*A. chinensis* (2×–6×), *A. eriantha*) and *S. tristyla*, representing the mitogenome structure. Genes drawn outside the circle are transcribed clockwise, and those inside are counterclockwise. Genes that belong to different functional groups are color coded. The darker grey in the inner circle indicates the GC content of the mitogenome.

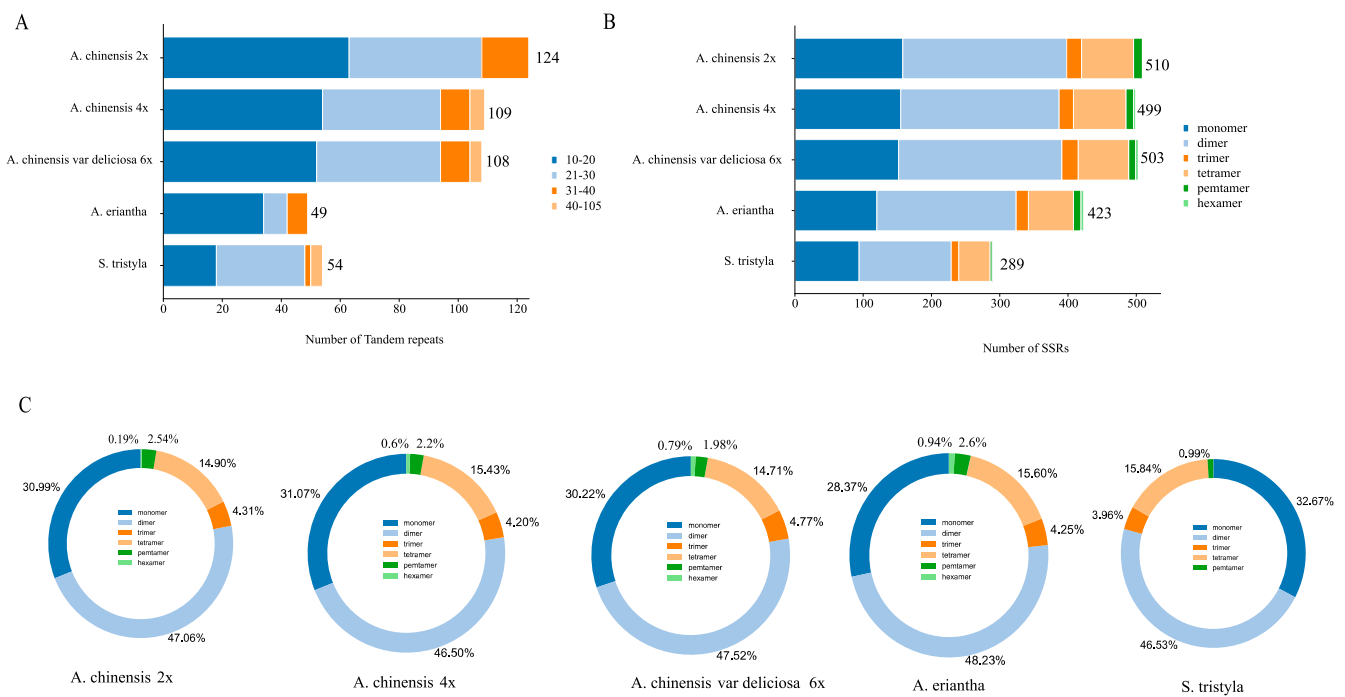


Figure 2. The tandem and SSR repeats in five Actiniaceae mitogenomes. (A) The number of tandem repeats. (B) The number of SSRs. (C) Pie chart for SSR distribution. The colors represent different types of SSRs.

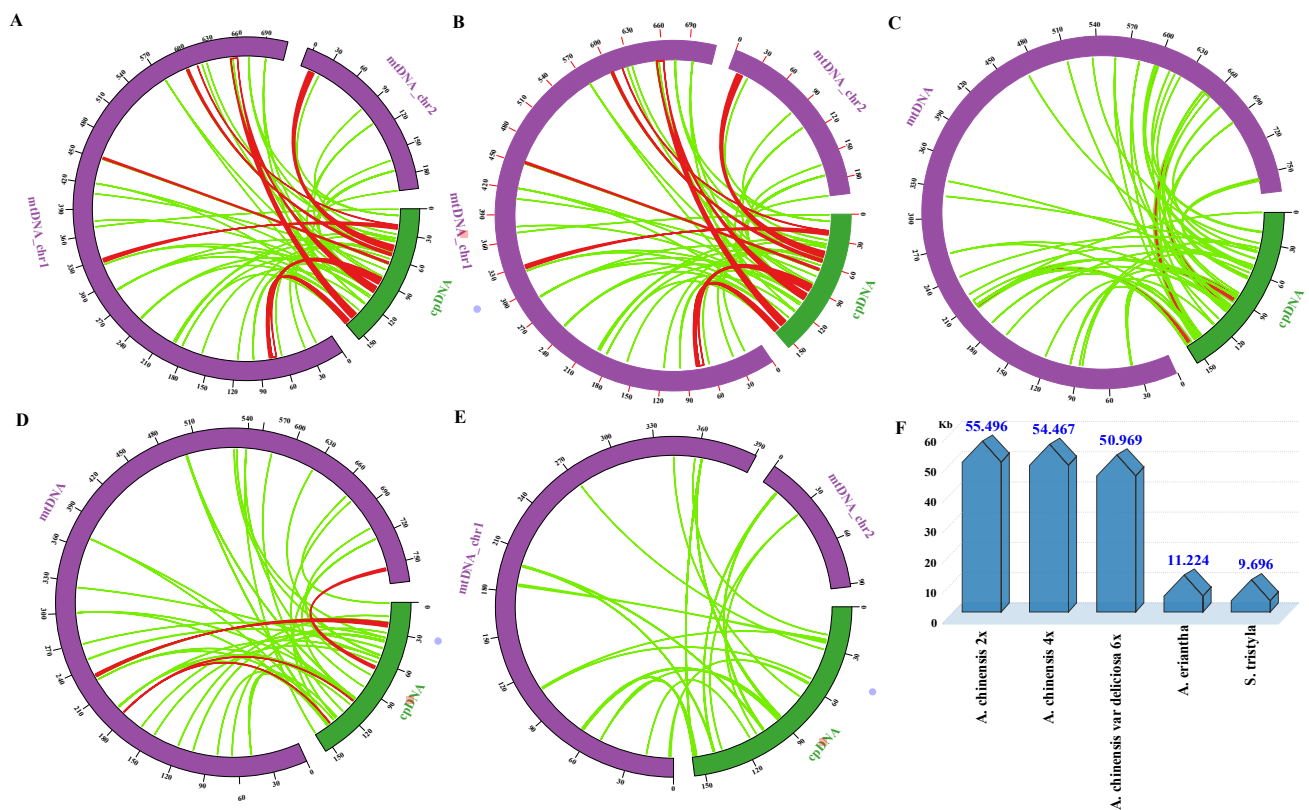


Figure 3. (A–E) Shared genome regions of each species between chloroplasts and mitochondria of *A. chinensis* (2×), *A. chinensis* (4×), *A. chinensis* var *deliciosa* (6×), *A. eriantha* and *S. tristyla*, respectively. The green circular segment represents the mitogenome, and the purple circular segment represents the chloroplast genome. (F) Shared sequence length of each species between chloroplasts and mitochondria genomes.

3.3. RNA Editing Sites and Codon Usage Analysis of PCGs

As shown in Figure 4, the RNA editing sites of 39 PCGs of the mitogenomes of 5 Actinidiaceae plants were predicted in this study. Three cytochrome c biogenesis genes, including *ccmFn*, *ccmB*, and *ccmC*, displayed the most RNA editing sites in five Actinaceae sp. plants. Interestingly, we found that the number of *NAD1* gene RNA editing sites in *A. chinensis* var *deliciosa* was significantly higher than in the other species (Figure 4). Only the *rpl2* gene in the *A. chinensis* (4×) had no RNA editing sites (Figure 4). The *rpl16*, *rps1*, and *rps2* genes contained the same number of editing sites in the *A. chinensis* (2×) and *A. eriantha*, but not in the other species (Figure 4).

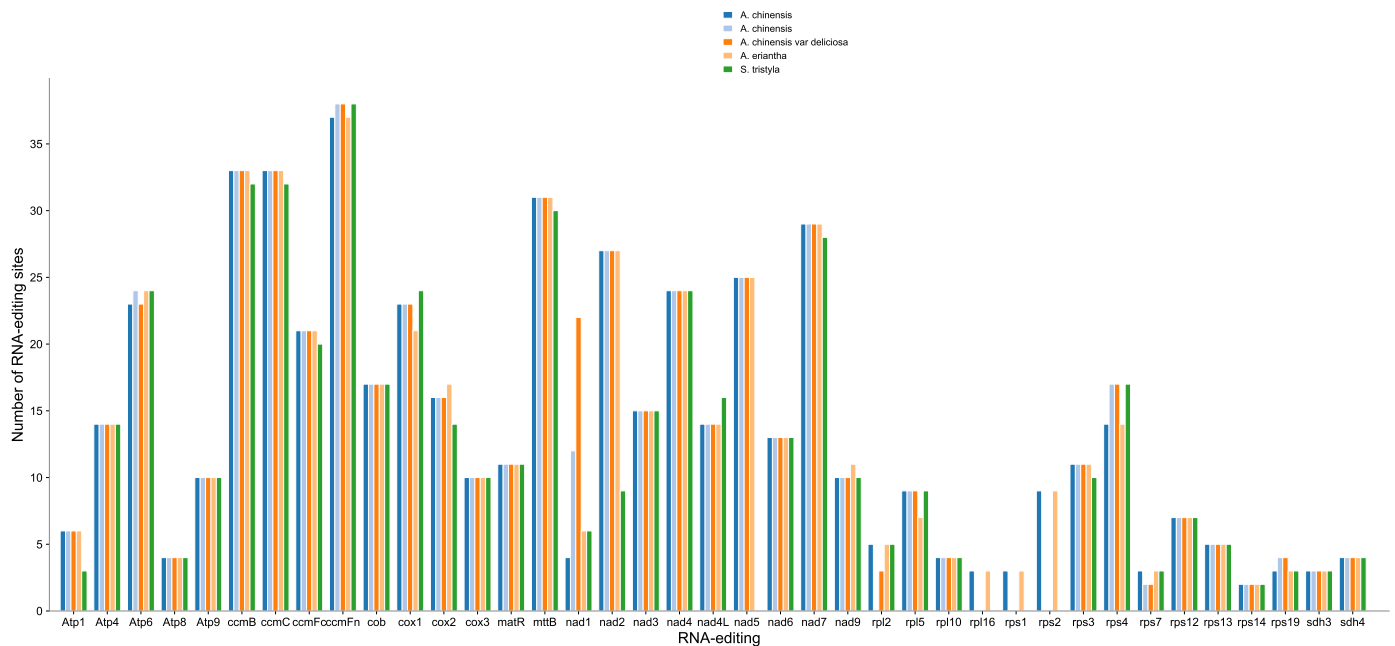


Figure 4. The distribution of RNA editing sites in mitogenome protein-coding genes.

The codon distribution and relative synonymous codon usage (RSCU) of five Actinidiaceae species' mitogenomes were analyzed. The RSCU analysis showed that Leu, Ser, and Arg appeared the most frequently, whereas those that encoded Met and Trp were relatively less abundant in five Actinidiaceae species' mitogenomes. Five species in the Actinidiaceae family share a similar RSCU style (Figure 5A–E).

3.4. The Synonymous and Nonsynonymous Substitution Rate (K_a/K_s) and Phylogenetic Analysis

Nineteen protein-coding genes of six Actinidiaceae mitogenomes were used to calculate the K_a/K_s ratios. As shown in Figure 6, we observed that the *sdh3* gene had an abnormally high K_a/K_s ratio > 1 compared to the other genes between *S. tristyla* and the kiwifruit, indicating possible positive selection. The K_a/K_s values of most PCGs were less than 1, such as *atp9*, *ccmB*, *ccmC*, *cox3*, *nad6* and *rps12*, indicating that most PCGs were under purification selection (Figure 6). These results suggested that most PCGs may be highly conservative in the evolutionary process of Actinidiaceae.

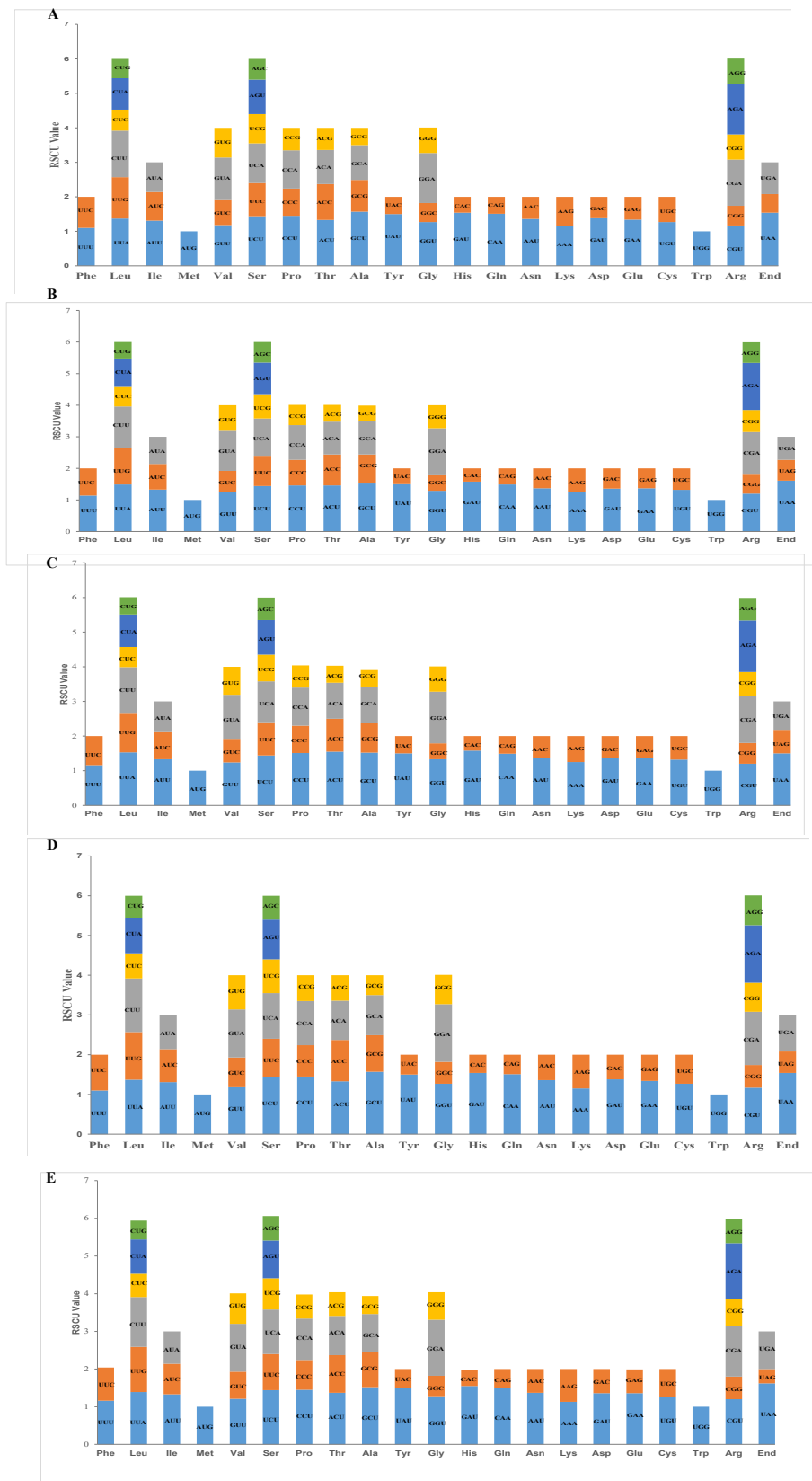


Figure 5. Relative synonymous codon usage (RSCU) in mitochondrial protein-coding genes of five *Actinidiaceae* mitogenomes. The y-axis represents the value for RSCU. (A) The RSCU value of *A. chinensis* (2×). (B) The RSCU value of *A. chinensis* (4×). (C) The RSCU value of *A. chinensis* var. *deliciosa* (6×). (D) The RSCU value of *A. eriantha*. (E) The RSCU value of *S. tristyla*.

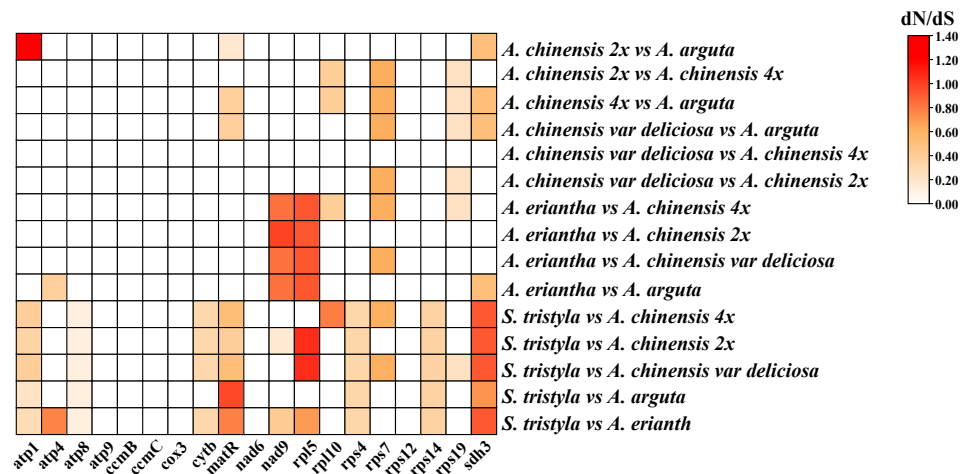


Figure 6. The pairwise Ka/Ks ratios among each mitochondrial gene in the six Actinidiaceae family species.

In order to further analyze the phylogenetic position of Actinidiaceae, 23 plant mitogenomes from GenBank were downloaded for phylogenetic tree construction based on 20 PCGs. Phylogenetic analysis showed that 23 plant mitogenomes were divided into 6 categories (Figure 7). We selected *V. vinifera* and *N. nucifera* as outgroups. The phylogenetic tree strongly demonstrated that five kiwifruit species (*A. chinensis* (2×), *A. chinensis* (4×), *A. chinensis* var *deliciosa* (6×), *A. eriantha* and *A. arguta*) clustered into one clade with a 100% bootstrap value (Figure 7). It also revealed that *S. tristyla* was closely related to five kiwifruit species (Figure 7).

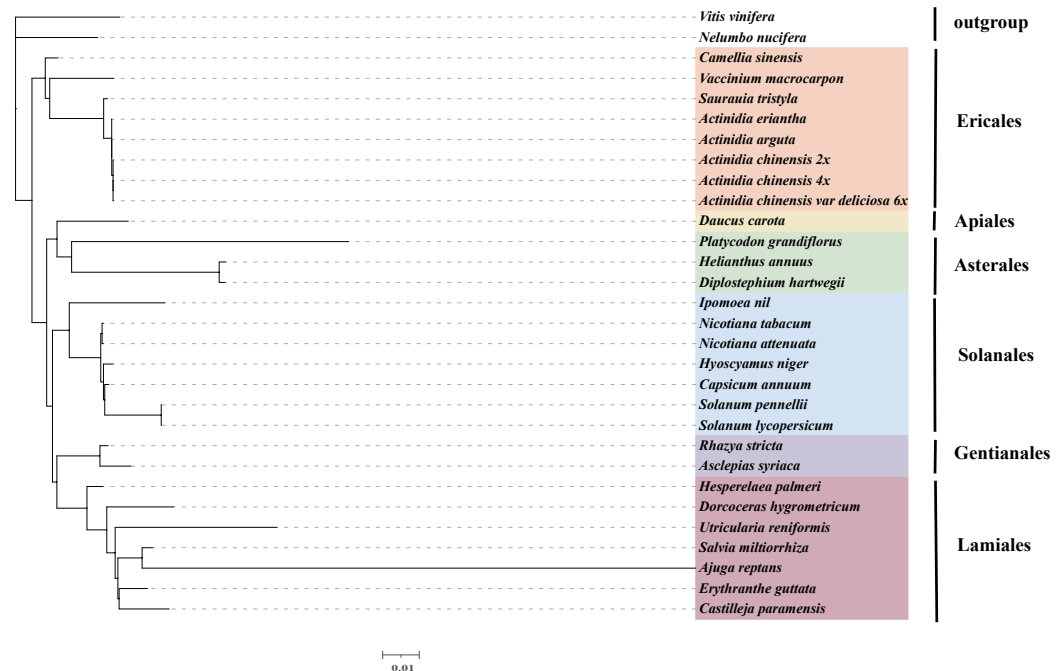


Figure 7. Maximum likelihood phylogenetic tree analysis of Actinidiaceae mitogenomes based on 20 PCGs of 23 plant mitogenomes with *V. vinifera* and *N. nucifera* as outgroups.

4. Discussion

So far, 25 *Actinidia* genus chloroplast genomes have been reported [32], and our group has comprehensively analyzed them. Unlike conserved genome structures and small *Actinidia* chloroplast genomes, *Actinidia* mitogenomes generally have multiple different sizes and

structural variations [55]. This makes *Actinidia* mitogenome research relatively challenging. Here, complete mitogenomes of five Actinidiaceae plants were sequenced and assembled. Two subgenomic circles were found in *A. chinensis* ($2\times-4\times$) and *S. tristyla*. Similar results have been reported in *C. sinensis* var. *assamica* and *C. assamica* [16,56]. The GC content of five *Actinidia* mitogenomes is about 46%, similar to most other mitogenomes [57]. Among the observed size variations, the genome size in *A. chinensis* var. *deliciosa* ($6\times$) was about twice that of the *S. tristyla* (482 kb) and the closely related species *Vaccinium macrocarpon* (459 kb) [58]. The genome size of the hexaploid *A. chinensis* var. *deliciosa* was nearly 20 kb larger than that of diploid and tetraploid *A. chinensis*, which is probably the result of a gradual increase in sequence duplication and intracellular transfer of the plastid or nuclear genome or horizontal transfer of mitochondrial DNA during evolution [59,60].

Repeat sequences widely exist in plant mitogenomes, including tandem repeats and SSRs [61]. Positive correlations between genome size and repeat sequences were identified in 38 Rosaceae mitogenomes [62]. As shown in Figure 2A, tandem repeats from 10 to 30 bp were the most abundant for the Actinidiaceae mitogenomes, with similar results in *Diospyros oleifera* [63]. Guo et al. [64] have reported that SSRs played a pivotal role in intermolecular recombination during evolution. The number of SSRs in the *A. chinensis* mitogenome (18.24%) was higher than that of *S. tristyla* and *A. eriantha* (Figure 2B), which may cause the *A. chinensis* mitogenome size to be larger than *S. tristyla* and *A. eriantha*. It is consistent with the findings of previous studies [65,66]. Dimer repeats were the most abundant SSR type (about 48%) in the *Actinidia* mitogenome (Figure 2C), which is commonly found in *Suaeda glauca* [67]. Gene transfer from the chloroplast to the mitogenome frequently occurs during long-term plant evolution [68]. A total of 9–55 kb of plastid-derived sequences was observed, which occupied 3–6% of the Actinidiaceae mitogenomes (Figure 3). Similar results have been reported by Adams et al. [69]. Some plastid-derived protein-coding genes (cp-derived PCGs), such as *rpoC1*, *ndhB*, *rps7*, *rps19*, and *rpl23*, were identified in the *A. chinensis* ($2\times-4\times$) mitogenomes, which is commonly found in angiosperms [70]. In addition, we also found that *psbJ*, *petL* and *petG* cp-derived genes only exist in hexaploid *A. chinensis* var. *deliciosa* (Supplementary Table S2), suggesting that special evolutionary events may have occurred during genome evolution.

Mitochondrial gene expression may be affected by RNA editing [71]. The number of RNA editing sites varies in different species [72]. Previous studies identified approximately 491 RNA editing sites within 34 genes in rice [68] and 486 RNA editing sites within 31 genes in *Primula vulgaris* [73]. In Actinidiaceae, the number of RNA editing sites in most PCGs was extremely conserved in Actinidiaceae, similar to other plant studies [74]. Interestingly, we also observed that the number of NAD1 gene RNA editing sites increased with ploidy in *A. chinensis* ($2\times-4\times$) (Figure 4). Whether the number of RNA editing sites is positively correlated with the ploidy of the kiwifruit requires further research. Relative synonymous codon usage (RSCU) refers to the relative probability of a specific codon between the synonymous codons that encode the corresponding amino acid [75]. The RSCU value showed that the codon usage pattern in the Actinidiaceae plants' mitogenomes shared a similar RSCU style (Figure 5A–E), which was commonly found in higher plant mitogenomes [76].

Calculating the Ka/Ks ratio plays a vital role in understanding the dynamics of molecular evolution [77]. As shown in Figure 6, the Ka/Ks ratios of most PCGs were less than 1 (Figure 6), suggesting that these genes were highly conserved and had undergone neutral and negative selections in Actinidiaceae. These results were also supported in the report on Lamiales [78]. However, among the five Actinidiaceae plants, *sdh3* with dN/dS values greater than 1.0 was found between the *S. tristyla* and kiwifruit mitogenomes, indicating that this gene may have suffered from positive selection during the evolution in Actinidiaceae. The phylogenetic trees in this study showed a close relationship between the Actinidiaceae and other Ericaceae plants (Figure 7), as Wang et al. [56] proposed. Notably, our analyses also demonstrated that the Actinidiaceae is monophyly, with the sampled five *Actinidia* taxa clustering in a clade as a sister to *S. tristyla* (Figure 7), in agreement with the

result of Wang et al. [32]. Moreover, *A. chinensis* (2×–4×) was closely related to *A. chinensis* var *deliciosa* (6×) (Figure 7), which was consistent with the results of a previous study [79].

5. Conclusions

The large size variation in Actinidiaceae mitogenomes appeared due to increasing sequence duplication and intracellular transfer of the plastid. The number of RNA editing sites and codon usage in most PCGs of five Actinidiaceae plants' mitogenomes were highly conserved. Most of the coding genes had undergone negative selection, indicating the conservation of mt genes during evolution. We found that *sdh3* may have suffered from positive selection during the evolution in Actinidiaceae. Kiwifruit species showed high similarities and were highly similar to *S. tristyla* and *A. chinensis* (2×–4×) was closely related to *A. chinensis* var *deliciosa* (6×). This study provides important mitochondrial genome resources for the Actinidiaceae species and has deepened our understanding of organelle genome evolution in flowering plants.

Supplementary Materials: The following supporting information can be downloaded at: <https://www.mdpi.com/article/10.3390/genes13101827/s1>. Table S1. Statistics information of sequenced land plant complete mitogenomes; Table S2. Features of five mitogenomes that belong to the Actiniaceae family; Table S3. Taxonomic information, GenBank accession numbers and collection place of mitogenomes used in the study; Figure S1. Statistics information of sequenced land plant complete mitogenomes from 1993 to 2022; Figure S2. Production quantities of kiwifruit by country; Figure S3. Yield quantities of kiwifruit in the world from 1999 to 2020; Figure S4. Production share of kiwifruits by region; Figure S5. Production of kiwifruit, including the top 10 producers.

Author Contributions: J.Y. designed the experiment, carried out the bioinformatic analyses, and wrote the first manuscript. J.Y., C.L. and Y.L. collected the plant materials. C.L. and H.Z. participated in carrying out some experiments. Q.H. and S.L. contributed to the result interpretation and manuscript revision and funding acquisition. J.Y., G.Z. and Y.L. conceived the experiments and revised the manuscript. All authors have read and agreed to the published version of the manuscript.

Funding: This work was supported by funds from the National Natural Science Foundation of China (31972474, 90717110).

Institutional Review Board Statement: Not applicable.

Informed Consent Statement: Not applicable.

Data Availability Statement: The accession number generated for this study can be found in Table S3.

Conflicts of Interest: The authors declare no conflict of interest.

References

1. Gray, M.W.; Burger, G.; Lang, B.F. Mitochondrial evolution. *Science* **1999**, *283*, 1476–1481. [[CrossRef](#)] [[PubMed](#)]
2. Gray, M.W.; Lang, B.F.; Burger, G. Mitochondria of protists. *Annu. Rev. Genet.* **2004**, *38*, 477–524. [[CrossRef](#)] [[PubMed](#)]
3. Sloan, D.B.; Wu, Z.; Sharbrough, J. Correction of persistent errors in Arabidopsis reference mitochondrial genomes. *Plant Cell* **2018**, *30*, 525–527. [[CrossRef](#)] [[PubMed](#)]
4. Ye, N.; Wang, X.; Li, J.; Bi, C.; Xu, Y.; Wu, D.; Ye, Q. Assembly and comparative analysis of complete mitochondrial genome sequence of an economic plant *Salix suchowensis*. *Peer J.* **2017**, *5*, e3148. [[CrossRef](#)] [[PubMed](#)]
5. Birky, C.W., Jr. Uniparental inheritance of mitochondrial and chloroplast genes: Mechanisms and evolution. *Proc. Natl. Acad. Sci. USA* **1995**, *92*, 11331–11338. [[CrossRef](#)] [[PubMed](#)]
6. Wu, Z.Q.; Liao, X.Z.; Zhang, X.N.; Tembrock, L.R.; Broz, A. Genomic architectural variation of plant mitochondria—A review of multichromosomal structuring. *J. Syst. Evol.* **2020**, *60*, 160–168. [[CrossRef](#)]
7. Cole, L.W.; Guo, W.; Mower, J.P.; Palmer, J.D. High and variable rates of repeat-mediated mitochondrial genome rearrangement in a genus of plants. *Mol. Biol. Evol.* **2018**, *35*, 2773–2785. [[CrossRef](#)] [[PubMed](#)]
8. Morley, S.A.; Nielsen, B.L. Plant mitochondrial DNA. *Molecules* **2017**, *15*, 17.
9. Bergthorsson, U.; Adams, K.L.; Thomason, B.; Palmer, J.D. Widespread horizontal transfer of mitochondrial genes in flowering plants. *Nature* **2003**, *424*, 197–201. [[CrossRef](#)]
10. Li, J.; Xu, Y.; Shan, Y.; Pei, X.; Yong, S.; Liu, C.; Yu, J. Assembly of the complete mitochondrial genome of an endemic plant, *Scutellaria tsinyunensis*, revealed the existence of two conformations generated by a repeat-mediated recombination. *Planta* **2021**, *254*, 36. [[CrossRef](#)]

11. Alverson, A.J.; Rice, D.W.; Dickinson, S.; Barry, K.; Palmer, J.D. Origins and recombination of the bacterial-sized multichromosomal mitochondrial genome of cucumber. *Plant Cell* **2011**, *23*, 2499–2513. [[CrossRef](#)] [[PubMed](#)]
12. Yang, Z.; Ni, Y.; Lin, Z.; Yang, L.; Chen, G.; Nijjati, N.; Hu, Y.; Chen, X. De novo assembly of the complete mitochondrial genome of sweet potato (*Ipomoea batatas* [L.] Lam) revealed the existence of homologous conformations generated by the repeat-mediated recombination. *BMC Plant Biol.* **2022**, *22*, 285. [[CrossRef](#)] [[PubMed](#)]
13. Sang, S.F.; Mei, D.S.; Liu, J.; Zaman, Q.U.; Zhang, H.Y.; Hao, M.Y.; Fu, L.; Wang, H.; Cheng, H.F.; Hu, Q. Organelle genome composition and candidate gene identification for Nsa cytoplasmic male sterility in *Brassica napus*. *BMC Genom.* **2019**, *20*, 813. [[CrossRef](#)] [[PubMed](#)]
14. Albert, V.A.; Jobson, R.W.; Michael, T.P.; Taylor, D.J. The carnivorous bladderwort (*Utricularia*, Lentibulariaceae): A system inflates. *J. Exp. Bot.* **2010**, *61*, 5–9. [[CrossRef](#)]
15. Phillips, W.S.; Brown, A.M.; Howe, D.K.; Peetz, A.B.; Blok, V.C.; Denver, D.R.; Zasada, I.A. The mitochondrial genome of *Globodera ellingtonae* is composed of two circles with segregated gene content and differential copy numbers. *BMC Genom.* **2016**, *17*, 706. [[CrossRef](#)]
16. Zhang, F.; Li, W.; Gao, C.W.; Zhang, D.; Gao, L.Z. Deciphering tea tree chloroplast and mitochondrial genomes of *Camellia sinensis* var. *assamica*. *Sci. Data* **2019**, *6*, 209. [[CrossRef](#)]
17. Richardson, A.O.; Rice, D.W.; Young, G.J.; Alverson, A.J.; Palmer, J.D. The “fossilized” mitochondrial genome of *Liriodendron tulipifera*: Ancestral gene content and order, ancestral editing sites, and extraordinarily low mutation rate. *BMC Biol.* **2013**, *11*, 29. [[CrossRef](#)]
18. Bi, C.; Paterson, A.H.; Wang, X.; Xu, Y.; Wu, D.; Qu, Y.; Jiang, A.; Ye, Q.; Ye, N. Analysis of the Complete mitochondrial genome sequence of the diploid cotton *Gossypium raimondii* by comparative genomics approaches. *BioMed Res. Int.* **2016**, *2016*, 5040598. [[CrossRef](#)]
19. Mwamuye, M.M.; Obara, I.; Elati, K.; Odongo, D.; Bakheit, M.A.; Jongejan, F. Unique mitochondrial single nucleotide polymorphisms demonstrate resolution potential to discriminate *Theileria parva* vaccine and buffalo-derived strains. *Life* **2020**, *10*, 334. [[CrossRef](#)]
20. Zhang, D.; Xing, Y.; Xu, L.; Zhao, R.; Yang, Y.; Zhang, T.; Li, S.; Bao, G.; Ao, W.; Liu, T. *Comparative analysis of the mitochondrial genome sequences of two medicinal plants: Arctium lappa and A. tomentosum*; Research Square: Durham, NC, USA, 2020.
21. Mower, J.P.; Sloan, D.B.; Alverson, A.J. Plant mitochondrial genome diversity: The genomics revolution. *Plant Genome Divers.* **2012**, *1*, 123–144.
22. Dietrich, A.; Maréchal-Drouard, L.; Carneiro, V.; Cosset, A.; Small, I. A single base change prevents import of cytosolic tRNA(Ala) into mitochondria in transgenic plants. *Plant J.* **1996**, *10*, 913–918. [[CrossRef](#)] [[PubMed](#)]
23. Ming, R.; Bendahmane, A.; Renner, S.S. Sex chromosomes in land plants. *Annu. Rev. Plant Biol.* **2011**, *62*, 485–514. [[CrossRef](#)] [[PubMed](#)]
24. Vanneste, J.L. The scientific, economic, and social impacts of the New Zealand outbreak of bacterial canker of kiwifruit (*Pseudomonas syringae* pv. *actinidiae*). *Annu. Rev. Phytopathol.* **2017**, *55*, 377–399. [[CrossRef](#)] [[PubMed](#)]
25. Sun, L.M.; Fang, J.B.; Zhang, M.; Qi, X.J.; Lin, M.M.; Chen, J.Y. Molecular cloning and functional analysis of the *NPR1* Homolog in kiwifruit (*Actinidia chinensis*). *Front. Plant Sci.* **2020**, *11*, 551201. [[CrossRef](#)] [[PubMed](#)]
26. Pan, D.L.; Wang, G.; Wang, T.; Jia, Z.H.; Guo, Z.R.; Zhang, J.Y. AdRAP2.3, a novel ethylene response factor VII from *Actinidia deliciosa*, enhances waterlogging resistance in transgenic tobacco through improving expression levels of PDC and ADH genes. *Int. J. Mol. Sci.* **2019**, *20*, 1189. [[CrossRef](#)] [[PubMed](#)]
27. Griffiths, L.M.; Swartzlander, D.; Meadows, K.L.; Wilkinson, K.D.; Corbett, A.H.; Doetsch, P.W. Dynamic compartmentalization of base excision repair proteins in response to nuclear and mitochondrial oxidative stress. *Mol. Cell. Biol.* **2009**, *29*, 794–807. [[CrossRef](#)]
28. Wu, H.; Ma, T.; Kang, M.; Ai, F.; Zhang, J.; Dong, G.; Liu, J. A high-quality *Actinidia chinensis* (kiwifruit) genome. *Hortic. Res.* **2019**, *6*, 117. [[CrossRef](#)]
29. Huang, S.; Ding, J.; Deng, D.; Tang, W.; Sun, H.; Liu, D.; Zhang, L.; Niu, X.; Zhang, X.; Meng, M.; et al. Draft genome of the kiwifruit *Actinidia chinensis*. *Nat. Commun.* **2013**, *4*, 2640. [[CrossRef](#)]
30. Tang, W.; Sun, X.; Yue, J.; Tang, X.; Jiao, C.; Yang, Y.; Niu, X.; Miao, M.; Zhang, D.; Huang, S.; et al. Chromosome-scale genome assembly of kiwifruit *Actinidia chinensis* with single-molecule sequencing and chromatin interaction mapping. *GigaScience* **2019**, *8*. [[CrossRef](#)]
31. Pilkington, S.M.; Crowhurst, R.; Hilario, E.; Nardoza, S.; Fraser, L.; Peng, Y.; Gunaseelan, K.; Simpson, R.; Tahir, J.; Derolles, S.C.; et al. A manually annotated *Actinidia chinensis* var. *chinensis* (kiwifruit) genome highlights the challenges associated with draft genomes and gene prediction in plants. *BMC Genom.* **2018**, *19*, 1–19. [[CrossRef](#)] [[PubMed](#)]
32. Wang, L.; Liu, B.; Yang, Y.; Zhuang, Q.; Chen, S.; Liu, Y.; Huang, S. The comparative studies of complete chloroplast genomes in *Actinidia* (*Actinidiaceae*): Novel insights into heterogenous variation, *clpP* gene annotation and phylogenetic relationships. *Mol. Genet. Genom.* **2022**, *297*, 535–551. [[CrossRef](#)] [[PubMed](#)]
33. Emerman, A.B.; Bowman, S.K.; Barry, A.; Henig, N.; Patel, K.M.; Gardner, A.F.; Hendrickson, C.L. NEBNext direct: A novel, rapid, hybridization-based approach for the capture and library conversion of genomic regions of interest. *Curr. Protoc. Mol. Biol.* **2017**, *119*, 7–30. [[CrossRef](#)] [[PubMed](#)]

34. Istace, B.; Friedrich, A.; d'Agata, L.; Faye, S.; Payen, E.; Beluche, O.; Caradec, C.; Davidas, S.; Cruaud, C.; Liti, G.; et al. De novo assembly and population genomic survey of natural yeast isolates with the Oxford Nanopore MinION sequencer. *GigaScience* **2017**, *6*, 1–13. [[CrossRef](#)]
35. Li, H. Minimap and minimap: Fast mapping and de novo assembly for noisy long sequences. *Bioinformatics* **2016**, *32*, 2103–2110. [[CrossRef](#)]
36. Vaser, R.; Sović, I.; Nagarajan, N.; Šikić, M. Fast and accurate de novo genome assembly from long uncorrected reads. *Genome Res.* **2017**, *27*, 737–746. [[CrossRef](#)]
37. Walker, B.J.; Abeel, T.; Shea, T.; Priest, M.; Abouelliel, A.; Sakthikumar, S.; Cuomo, C.A.; Zeng, Q.; Wortman, J.; Ypung, S.K.; et al. Pilon: An integrated tool for comprehensive microbial variant detection and genome assembly improvement. *PLoS ONE* **2014**, *9*, e112963. [[CrossRef](#)]
38. Li, H.; Durbin, R. Fast and accurate short read alignment with Burrows-Wheeler transform. *Bioinformatics* **2009**, *25*, 1754–1760. [[CrossRef](#)]
39. Li, H.; Handsaker, B.; Wysoker, A.; Fennell, T.; Ruan, J.; Homer, N.; Marth, G.; Abecasis, G.; Durbin, R.; 1000 Genome Project Data Processing Subgroup. The sequence alignment/map format and SAMtools. *Bioinformatics* **2009**, *25*, 2078–2079. [[CrossRef](#)]
40. Tillich, M.; Lehwark, P.; Pellizzer, T.; Ulbricht-Jones, E.S.; Fischer, A.; Bock, R.; Greiner, S. GeSe-versatile and accurate annotation of organelle genomes. *Nucleic Acids Res.* **2017**, *45*, w6–w11. [[CrossRef](#)]
41. Misra, S.; Harris, N. Using Apollo to browse and edit genome annotations. *Curr. Protoc. Bioinformatics* **2006**, *12*, 9-5. [[CrossRef](#)] [[PubMed](#)]
42. Greiner, S.; Lehwark, P.; Bock, R. OrganellarGenomeDRAW (OGDRAW) version 1.3.1: Expanded toolkit for the graphical visualization of organellar genomes. *Nucleic Acids Res.* **2019**, *47*, w59–w64. [[CrossRef](#)] [[PubMed](#)]
43. Chan, P.P.; Lowe, T.M. tRNAscan-SE: Searching for tRNA genes in genomic sequences. *Methods Mol. Biol.* **2019**, *1962*, 1–14. [[PubMed](#)]
44. Beier, S.; Thiel, T.; Münch, T.; Scholz, U.; Mascher, M. MISA-web: A web server for microsatellite prediction. *Bioinformatics* **2017**, *33*, 2583–2585. [[CrossRef](#)]
45. Benson, G. Tandem repeats finder: A program to analyze DNA sequences. *Nucleic Acids Res.* **1999**, *27*, 573–580. [[CrossRef](#)]
46. Chen, Y.; Ye, W.; Zhang, Y.; Xu, Y. High speed BLASTN: An accelerated MegaBLAST search tool. *Nucleic Acids Res.* **2015**, *43*, 7762–7768. [[CrossRef](#)]
47. Chen, C.J.; Chen, H.; Zhang, Y.; Thomas, H.R.; Frank, M.H.; He, Y.H.; Xia, R. TBtools: An integrative toolkit developed for interactive analyses of big biological data. *Mol. Plant* **2020**, *13*, 1194–1202. [[CrossRef](#)]
48. Mower, J.P. The PREP suite: Predictive RNA editors for plant mitochondrial genes, chloroplast genes and user-defined alignments. *Nucleic Acids Res.* **2009**, *37*, w253–w259. [[CrossRef](#)]
49. Kumar, S.; Stecher, G.; Li, M.; Knyaz, C.; Tamura, K. MEGA X: Molecular evolutionary genetics analysis across computing platforms. *Mol. Biol. Evol.* **2018**, *35*, 1547–1549. [[CrossRef](#)]
50. Yang, Z. PAML 4: Phylogenetic analysis by maximum likelihood. *Mol. Biol. Evol.* **2007**, *24*, 1586–1591. [[CrossRef](#)]
51. Zhang, D.; Gao, F.; Jakovlic, I.; Zou, H.; Zhang, J.; Li, W.X.; Wang, G.T. PhyloSuite: An integrated and scalable desktop platform for streamlined molecular sequence data management and evolutionary phylogenetics studies. *Mol. Ecol. Resour.* **2020**, *20*, 348–355. [[CrossRef](#)] [[PubMed](#)]
52. Rozewicki, J.; Li, S.; Amada, K.M.; Standley, D.M.; Katoh, K. MAFFT-DASH: Integrated protein sequence and structural alignment. *Nucleic Acids Res* **2019**, *47*, w5–w10. [[CrossRef](#)] [[PubMed](#)]
53. Stamatakis, A. RAxML version 8: A tool for phylogenetic analysis and post-analysis of large phylogenies. *Bioinformatics* **2014**, *30*, 1312–1313. [[CrossRef](#)] [[PubMed](#)]
54. Letunic, I.; Bork, P. Interactive tree of life (iTOL) v3: An online tool for the display and annotation of phylogenetic and other trees. *Nucleic Acids Res* **2016**, *44*, w242–w245. [[CrossRef](#)]
55. Wang, S.; Li, D.; Yao, X.; Song, Q.; Wang, Z.; Zhang, Q.; Zhong, C.; Liu, Y.; Huang, H. Evolution and diversification of kiwifruit mitogenomes through extensive whole-genome rearrangement and mosaic loss of intergenic sequences in a highly variable region. *Genome Biol. Evol.* **2019**, *11*, 1192–1206. [[CrossRef](#)]
56. Rawal, H.C.; Kumar, P.M.; Bera, B.; Singh, N.K.; Mondal, T.K. Decoding and analysis of organelle genomes of Indian tea (*Camellia assamica*) for phylogenetic confirmation. *Genomics* **2020**, *112*, 659–668. [[CrossRef](#)]
57. Zhao, N.; Wang, Y.; Hua, J. The roles of mitochondrion in intergenomic gene transfer in plants: A source and a pool. *Int. J. Mol. Sci.* **2018**, *19*, 547. [[CrossRef](#)]
58. Diaz-Garcia, L.; Rodriguez-Bonilla, L.; Rohde, J.; Smith, T.; Zalapa, J. Pacbio sequencing reveals identical organelle genomes between American cranberry (*Vaccinium macrocarpon* Ait.) and a wild relative. *Genes* **2019**, *10*, 291. [[CrossRef](#)]
59. Zhao, N.; Grover, C.E.; Chen, Z.; Wendel, J.F.; Hua, J. Intergenomic gene transfer in diploid and allopolyploid *Gossypium*. *BMC Plant Biol.* **2019**, *19*, 492. [[CrossRef](#)]
60. Lonsdale, D.M. A review of the structure and organization of the mitochondrial genome of higher plants. *Plant Mol. Biol.* **1984**, *3*, 201–206. [[CrossRef](#)]
61. Xu, Y.; Cheng, W.; Xiong, C.; Jiang, X.; Wu, K.; Gong, B. Genetic diversity and association analysis among germplasms of diospyros kaki in Zhejiang province Based on SSR Markers. *Forests* **2021**, *12*, 422. [[CrossRef](#)]

62. Sun, M.; Zhang, M.; Chen, X.; Liu, Y.; Liu, B.; Li, J.; Wang, R.; Zhao, K.; Wu, J. Rearrangement and domestication as drivers of Rosaceae mitogenome plasticity. *BMC Biol.* **2022**, *20*, 181. [[CrossRef](#)] [[PubMed](#)]
63. Xu, Y.; Dong, Y.; Cheng, W.; Wu, K.; Gao, H.; Liu, L.; Xu, L.; Gong, B. Characterization and phylogenetic analysis of the complete mitochondrial genome sequence of *Diospyros oleifera*, the first representative from the family Ebenaceae. *Heliyon* **2022**, *8*, e09870. [[CrossRef](#)] [[PubMed](#)]
64. Guo, W.; Grewe, F.; Fan, W.; Young, G.J.; Knoop, V.; Palmer, J.D.; Mower, J.P. Ginkgo and Welwitschia mitogenomes reveal extreme contrasts in gymnosperm mitochondrial evolution. *Mol. Biol. Evol.* **2016**, *33*, 1448–1460. [[CrossRef](#)]
65. Orton, L.M.; Fitzek, E.; Feng, X.; Grayburn, W.S.; Mower, J.P.; Liu, K.; Zhang, C.; Duvall, M.R.; Yin, Y. *Zygnema circumcarinatum* UTEX 1559 chloroplast and mitochondrial genomes provide insight into land plant evolution. *J. Exp. Bot.* **2020**, *71*, 3361–3373. [[CrossRef](#)]
66. Xue, J.Y.; Wang, Y.; Chen, M.; Dong, S.; Shao, Z.Q.; Liu, Y. Maternal Inheritance of U's Triangle and Evolutionary Process of Brassica Mitochondrial Genomes. *Front. Plant Sci.* **2020**, *11*, 805.
67. Cheng, Y.; He, X.; Priyadarshani, S.V.G.N.; Wang, Y.; Ye, L.; Shi, C.; Ye, K.; Zhou, Q.; Luo, Z.; Deng, F.; et al. Assembly and comparative analysis of the complete mitochondrial genome of *Suaeda glauca*. *BMC Genom.* **2021**, *22*, 167. [[CrossRef](#)]
68. Niu, Y.; Gao, C.; Liu, J. Complete mitochondrial genomes of three Mangifera species, their genomic structure and gene transfer from chloroplast genomes. *BMC Genom.* **2022**, *23*, 147. [[CrossRef](#)]
69. Adams, K.L.; Qiu, Y.L.; Stoutemyer, M.; Palmer, J.D. Punctuated evolution of mitochondrial gene content: High and variable rates of mitochondrial gene loss and transfer to the nucleus during angiosperm evolution. *Proc. Natl. Acad. Sci. USA* **2002**, *99*, 9905–9912. [[CrossRef](#)]
70. Pinard, D.; Myburg, A.A.; Mizrahi, E. The plastid and mitochondrial genomes of *Eucalyptus grandis*. *BMC Genom.* **2019**, *20*, 132. [[CrossRef](#)]
71. Lukeš, J.; Kaur, B.; Spejjer, D. RNA Editing in Mitochondria and Plastids: Weird and Widespread. *Trends Genet.* **2021**, *37*, 99–102. [[CrossRef](#)] [[PubMed](#)]
72. Small, I.D.; Schallenberg-Rüdinger, M.; Takenaka, M.; Mireau, H.; Ostersezer-Biran, O. Plant organellar RNA editing: What 30 years of research has revealed. *Plant J.* **2020**, *101*, 1040–1056. [[CrossRef](#)] [[PubMed](#)]
73. Monnens, M.; Thijs, S.; Briscoe, A.G.; Clark, M.; Frost, E.J.; Littlewood, D.T.J.; Sewell, M.; Smeets, K.; Artois, T.; Vanhove, M.P.M. The first mitochondrial genomes of endosymbiotic rhabdocoels illustrate evolutionary relaxation of *atp8* and genome plasticity in flatworms. *Int. J. Biol. Macromol.* **2020**, *162*, 454–469. [[CrossRef](#)] [[PubMed](#)]
74. Gerke, P.; Szövényi, P.; Neubauer, A.; Lenz, H.; Gutmann, B.; McDowell, R.; Small, I.; Schallenberg-Rüdinger, M.; Knoop, V. Towards a plant model for enigmatic U-to-C RNA editing: The organelle genomes, transcriptomes, editomes and candidate RNA editing factors in the hornwort *Anthoceros agrestis*. *New Phytol* **2020**, *225*, 1974–1992. [[CrossRef](#)] [[PubMed](#)]
75. Zhou, M.; Li, X. Analysis of synonymous codon usage patterns in different plant mitochondrial genomes. *Mol. Biol. Rep.* **2009**, *36*, 2039–2046. [[CrossRef](#)] [[PubMed](#)]
76. Sloan, D.B.; Alverson, A.J.; Chuckalovcak, J.P.; Wu, M.; McCauley, D.E.; Palmer, J.D.; Taylor, D.R. Rapid evolution of enormous, multichromosomal genomes in flowering plant mitochondria with exceptionally high mutation rates. *PLoS Biol.* **2012**, *10*, e1001241. [[CrossRef](#)] [[PubMed](#)]
77. Li, J.; Zhang, Z.; Vang, S.; Yu, J.; Wong, G.K.; Wang, J. Correlation between Ka/Ks and Ks is related to substitution model and evolutionary lineage. *J. Mol. Evol.* **2009**, *68*, 414–423. [[CrossRef](#)]
78. Yu, X.; Duan, Z.; Wang, Y.; Zhang, Q.; Li, W. Sequence analysis of the complete mitochondrial genome of a medicinal Plant, *vitex rotundifolia* Linnaeus f. (Lamiales: Lamiaceae). *Genes* **2022**, *13*, 839. [[CrossRef](#)]
79. Wang, W.C.; Chen, S.Y.; Zhang, X.Z. Chloroplast genome evolution in Actinidiaceae: *clpP* loss, heterogenous divergence and phylogenomic practice. *PLoS ONE* **2016**, *11*, e0162324. [[CrossRef](#)]